PFC/JA-91-19

Experimental Study of a 33.3 GHZ Free Electron Laser Amplifier with a Reversed Axial Guide Magnetic Field

Conde, M.E. and Bekefi, G.

July, 1991

Plasma Fusion Center
Massachusetts Institute of Technology
Cambridge, MA 02139 USA

This work was supported by DOE, AFOSR and CNPq (Brazil). Reproduction, translation, publication, use and disposal, in whole of part, by or for the United States government is permitted.

Submitted for publication in Physical Review Letters.

Experimental Study of a 33.3 GHz Free Electron Laser Amplifier with a Reversed Axial Guide Magnetic Field

M.E. Conde and G. Bekefi

Department of Physics and Research Laboratory of Electronics
Massachusetts Institute of Technology
Cambridge, MA 02139

ABSTRACT

We report on a new regime of free electron laser operation with reversed axial guide magnetic field, in which the cyclotron rotation of the electrons in the uniform axial field opposes the rotation in the helical wiggler field. The 33.3 GHz free electron laser amplifier is driven by a mildly relativistic electron beam (750 kV, 300 A, 30 ns) and generates 61 MW of radiation with a 27% conversion efficiency. The results are compared with those obtained when the axial guide field is in its conventional orientation where considerable loss of power and efficiency is observed.

PACS numbers: 42.55.Tb, 52.75.Ms

The free electron laser (FEL) operating in a combined axial guide magnetic field and a helical wiggler field has been studied experimentally[1,2] and theoretically[3] over a period of many years, both in linear and nonlinear regimes. In all these studies, the axial magnetic field $\mathbf{B}_z$ is oriented so that the cylotron rotation of the beam electrons is in the same direction as the rotation imposed by the helical wiggler field $\mathbf{B}_w$. This leads to an increase[4,5,6] of the transverse electron velocity $v_\perp$ compared to what it would be in the absence of $\mathbf{B}_z$, with potential benefits such as an enhanced radiation growth rate and efficiency.[3] Indeed, when the cyclotron wavelength in the axial field $\lambda_c = 2\pi v_z/\Omega_z$, approaches the wiggler periodicity l_w the transverse electron excursions can become too large, the electrons strike the drift tube wall and are lost ($\Omega_z = eB_z/m_0\gamma$ is the cyclotron frequency in the guide field and $\gamma = [1-(v_z/c)^2-(v_\perp/c)^2]^{-1/2}$ is the relativistic energy factor). Thus, the "resonance" $\lambda_c = l_w$ becomes a dividing line for conventional FEL operation: at relatively weak axial fields, $\lambda_c > l_w$, we have the so called Group I regime, and for stronger fields such that $\lambda_c < l_w$, the Group II regime.

In this letter we report measurements using a new, hitherto unexplored configuration with a reversed axial magnetic field. The electron rotations in the $\mathbf{B}_z$ and $\mathbf{B}_w$ fields now oppose one another, there is no longer the resonance at $\lambda_c = l_w$, and the transverse electron velocity $v_\perp$ is diminished compared to what it would be in the absence of $\mathbf{B}_z$ (however, the latter reduction is readily compensated in our experiments by increasing B_w). We will show that a reversal of $\mathbf{B}_z$ yields higher radiation intensity and efficiency compared to what we were able to achieve with the conventional orientation of the axial magnetic field.

The three regimes of FEL operation (Group I, Group II, and Reversed Field) are displayed in Fig. 1 based on a particle trajectory calculation of v_z/c which neglects space charge and radiation, and assumes that the electrons are undergoing ideal helical orbits in the combined $\mathbf{B}_z$ and $\mathbf{B}_w$ fields. The solid points illustrate the three parameter regimes of B_z where maximum radiation has been observed in our experiments.

A schematic of the FEL amplifier is shown in Fig. 2. A mildly relativistic electron beam (750 $\pm$ 50 keV) is generated by a Marx capacitor bank (Physics International Pulserad 110 A). The electrons are emitted from a hemispherical graphite cathode by an explosive field emission process. The graphite anode acts as an emittance selector, allowing only a small fraction of the current to propagate through its 2.54 mm radius and 62 mm long aperture. The electron beam current downstream from the emittance selector is illustrated in Fig. 3, showing saturation at high B_z where all available electrons from the gun have made it through the anode hole. From such measurements we are able to estimate the normallized RMS beam emittance $\epsilon_n < 4.4 \times 10^{-2}$ cm-rad and the corresponding RMS axial energy spread $\Delta\gamma_z/\gamma_z < 1.5 \times 10^{-2}$. We observe from Fig. 3b that when the wiggler is turned on, an expected very pronounced current loss occurs near resonance $\lambda_c = l_w$ with the conventional orientation of $\mathbf{B}_z$, but no significant current loss (also as expected), with the magnetic field reversed (Fig. 3c).

The 50 period bifilar helical wiggler produced by current carrying helical wires has a period of 3.18 cm and provides a magnetic field whose magnitude on axis is adjustable up to 1.8 kG. The wiggler field is slowly up-tapered over the initial six periods, providing an adiabatic input for the electron beam. The system, including

the gun, is immersed in a uniform axial magnetic field generated by a solenoid. The intensity of this field can be varied up to a maximum of 11.6 kG.

The 2 meter long stainless steel drift tube has an internal radius of 0.51 cm and acts as a cylindrical waveguide whose fundamental TE_{11} mode has a cutoff frequency of 17.2 GHz. The system is designed to operate in this lowest waveguide mode.

A high power magnetron operating at 33.39 GHz is the input power source for the FEL amplifier. The wave launcher consists of a short section of circular waveguide of radius 0.31 cm into which 17 kW are coupled from a standard Ka-band rectangular waveguide. This section of circular waveguide supports only the fundamental TE_{11} mode for the operating frequency. Its radius is then adiabatically up-tapered to the radius of the drift tube. A linearly polarized wave is thereby injected into the interaction region. Half of the incident power, with the correct rotation of the electric field vector, participates in the FEL interaction.

The output power from the FEL is transmitted by means of a conical horn into a reflection free "anechoic chamber". A small fraction of the radiation is then collected by a receiving horn, passes through precision calibrated attenuators, and a 1.7 GHz wide band pass filter. The power level is finally determined from the response of a calibrated crystal detector. The entire system is calibrated absolutely by a substitution method, i.e., by turning off the electron beam and measuring the received power in terms of the known input power from the magnetron.

Angular scans of the radiation pattern of the transmitting horn carried out within the anechoic chamber, together with a set of high pass waveguide filters are used to

confirm that the FEL indeed operates in the TE_{11} waveguide mode. The frequency spectrum of the output power has also been determined by a heterodyne technique (see Fig. 2). A crystal rectifier is used as a mixer for the 33 GHz FEL radiation and for radiation from a variable frequency 23 GHz local oscillator. The beat wave is amplified by a TWT amplifier and sent into a filter bank, composed of 13 channels adjacent in frequency, each 80 MHz wide. Thus, on a single shot basis, the radiation frequency is determined to be 33.39 GHz with a full width at half maximum of less than 160 MHz.

A parameter scan of the output power has been carried out in order to discover the optimum operating conditions for our three regimes, Group I, Group II and Reversed Field. Figure 4a illustrates the output power as a function of B_w at constant B_z, and Figs. 4b and 4c show how the power varies with B_z at constant B_w. It is seen that the maximum output power obtained in Group I and Group II regimes is approximately the same, 5 MW; however, the efficiency is much higher for the Group I regime since here the beam current is smaller. The output power for the reversed field case is higher by an order of magnitude and reaches a level of 61 MW.

The spatial growth rate of the electromagnetic wave is determined from the measurement of the output power as a function of the length of the interaction region. This length is varied by changing the distance that the electron beam is allowed to propagate in the drift tube. Application of a strong magnetic field is sufficient to deflect the electrons into the waveguide wall and thereby terminate the interaction at that point. Figure 5 shows the result of this measurement for the three different regimes. The Group I regime has the highest small signal growth rate (44 dB/m) but the power

level reaches saturation at an efficiency of 9%. Operation in Group II shows the lowest growth rate (38 dB/m) and the lowest efficiency (2%). The Reversed Field operation has an intermediate growth rate (41 dB/m) but by far the highest efficiency (27%), and exhibits no power saturation.

In conclusion, we have found that our free electron laser shows highest efficiency and highest power output when operated with reversed axial guide magnetic field. Table I summarizes our findings. We believe that the 27% efficiency of our system exceeds the efficiency of previous FELs with untapered wigglers. If the $\sim$ 1 dB/m attenuation due to the stainless steel waveguide were subtracted from the measurements, the power and efficiency could be substantially higher. Moreover, Fig. 5c shows that our wiggler is too short to reach saturation, and much higher efficiency may well be possible with longer and/or tapered magnetic fields.

We note that our FEL falls into the so called Raman parameter regime where RF space charge effects must be allowed for, both in order to account for the radiation frequency and the power output. A detailed theoretical understanding of the Reversed Field FEL is as yet unavailable due in part to some lack of understanding of the electron trajectories themselves. This is clearly shown in Fig. 4c, where a large, unexpected dip in output power occurs near the "resonance" $\lambda_c \simeq l_w$, but no such dip occurs in the electron current (Fig. 3c). Thus, the ideal orbit model on which Fig. 1 is based may well need substantial modification when $\mathbf{B}_z$ is reversed from its usual orientation.

This study was supported by DOE, AFOSR and CNPq (Brazil). We thank I. Mastovsky, C.J. Taylor and T. Mizuno for the assistance in the experimental work.

Table I. Summary of experimental results.

PARAMETER	GROUP I	GROUP II	REVERSED FIELD
Frequency (GHz)	33.39	33.39	33.39
Beam energy (keV)	750	750	750
Beam current (A)	90	300	300
Guide field (kG)	4.06	10.9	-10.9
Wiggler field (kG)	0.63	0.63	1.47
Growth rate (dB/m)	44	38	41
Output power (MW)	5.8	4.2	61
Efficiency (%)	9	2	27

REFERENCES

[1] S.H. Gold, D.L. Hardesty, A.K. Kirkead, L.R. Barnett and V.L. Granatstein, *Phys. Rev. Lett.* **52**, 1218 (1984).

[2] J. Fajans, J.S. Wurtele, G. Bekefi, D.S. Knowles and K. Xu, *Phys. Rev. Lett.* **57**, 579 (1986); also, J. Fajans, G. Bekefi, Y.Z. Yin and B. Lax, *Phys. Fluids* **28**, 1995 (1985).

[3] A.K. Ganguly and H.P. Freund, *IEEE Trans. Plasma Sci.* **16**, 167 (1988).

[4] L. Friedland, *Phys. Fluids* **23**, 2376 (1980).

[5] P. Diament, *Phys. Rev. A* **23**, 2537 (1981).

[6] H.P. Freund and A.K. Ganguly, *IEEE J. Quantum Electron.* **QE-21**, 1073 (1985).

FIGURE CAPTIONS

FIG. 1. Ideal equilibrium electron orbits calculated for two different values of wiggler magnetic field. The solid points show the values of B_z where maximum power is observed for Group I, Group II and Reversed Field regimes.

FIG. 2. Free electron laser experimental setup.

FIG. 3. Electron beam current in the FEL as a function of the axial guide magnetic field B_z; (a) no wiggler magnetic field; (b) wiggler field B_w = 630 G and B_z in the conventional direction; (c) wiggler field B_w = 1.47 kG and B_z in the reversed direction.

FIG. 4. FEL output power as a function of B_z and B_w; (a) B_w scan for fixed B_z = 10.9 kG in each direction; (b) B_z scan in the conventional direction for fixed B_w = 630 G; (c) B_z scan in the reversed direction for fixed B_w = 1.47 kG.

FIG. 5. FEL output power as a function of interaction length; (a) Group I regime; (b) Group II regime; (c) Reversed Field regime.

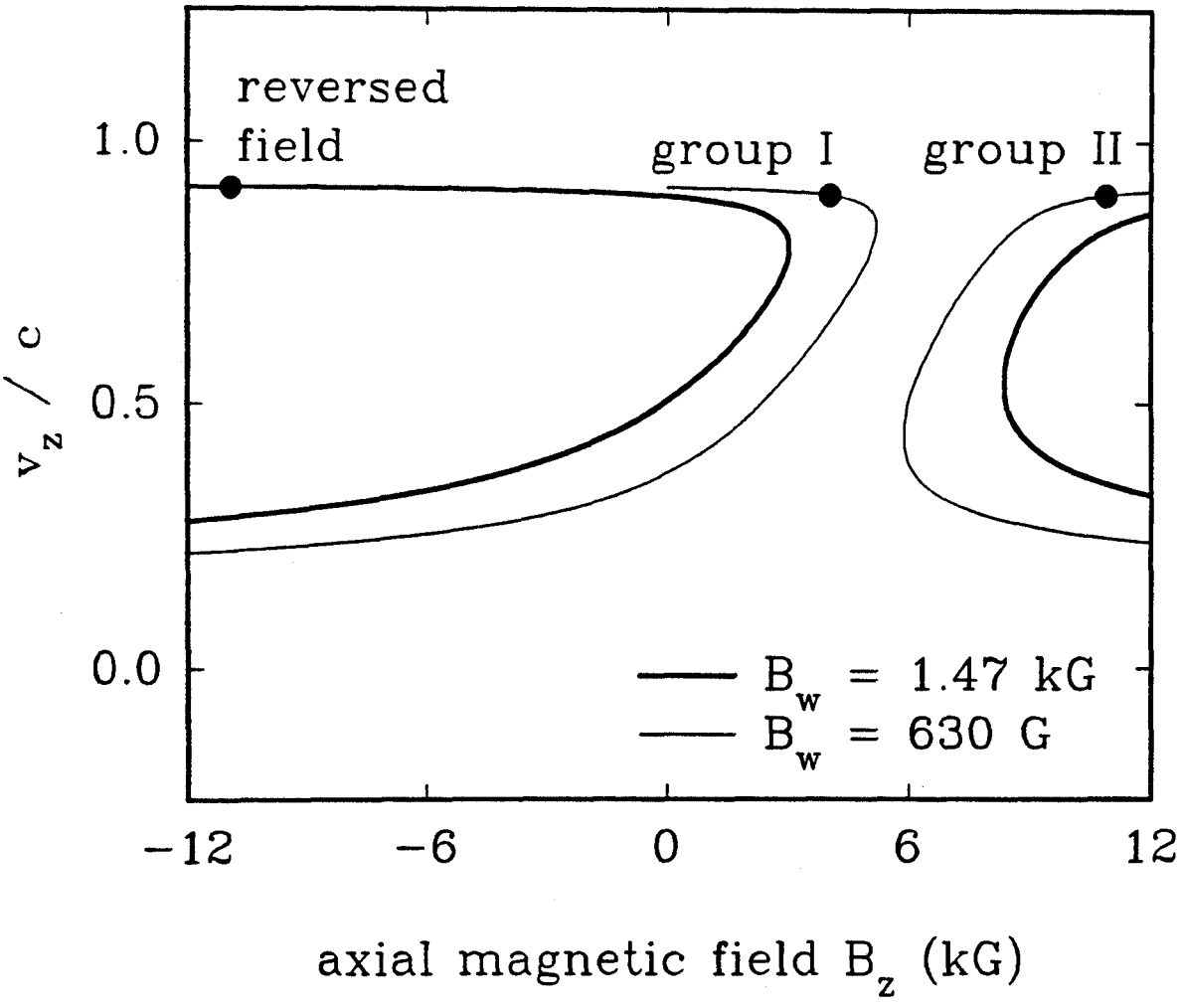

Fig.1 Conde and Bekefi

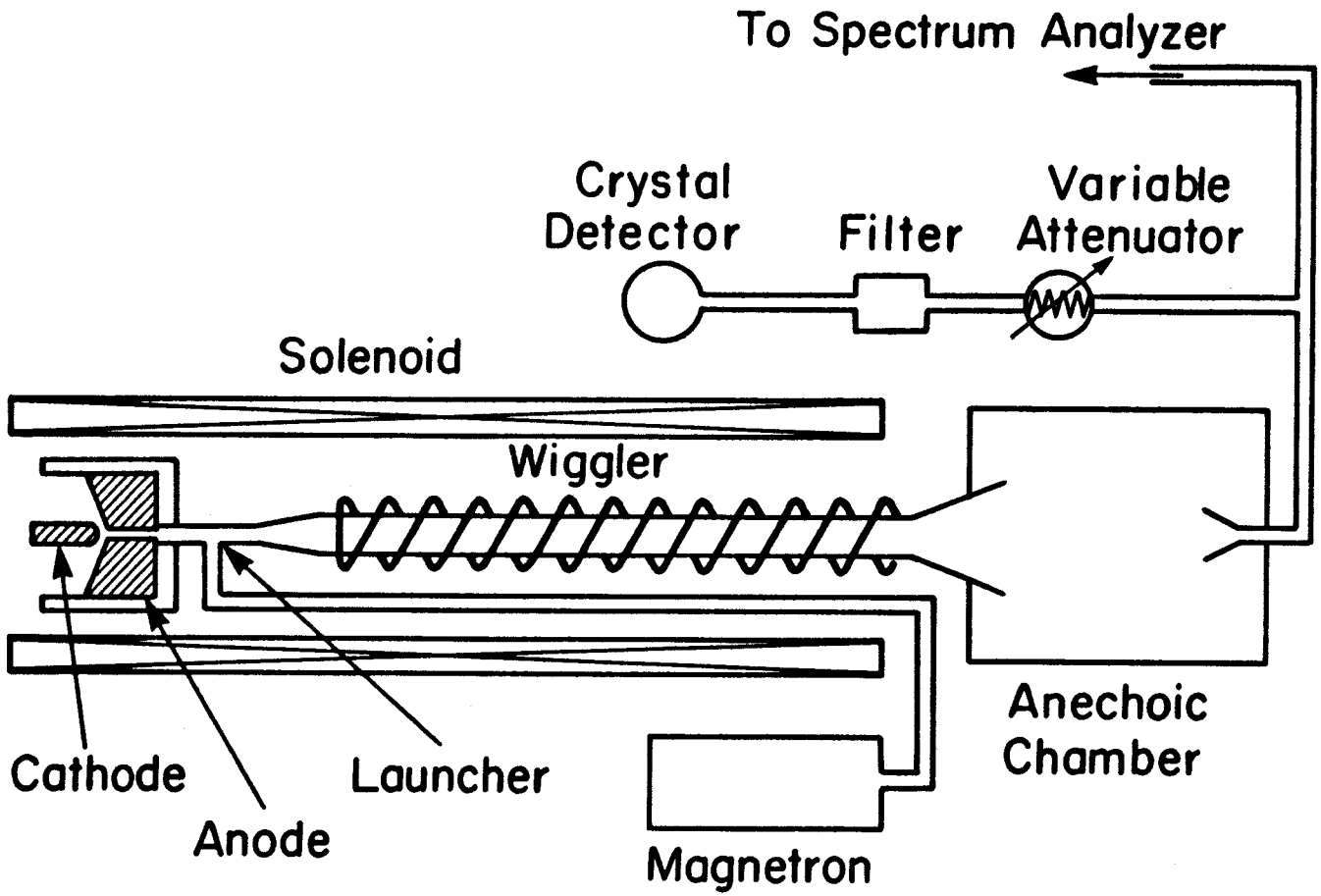

Fig.2 Conde and Bekefi

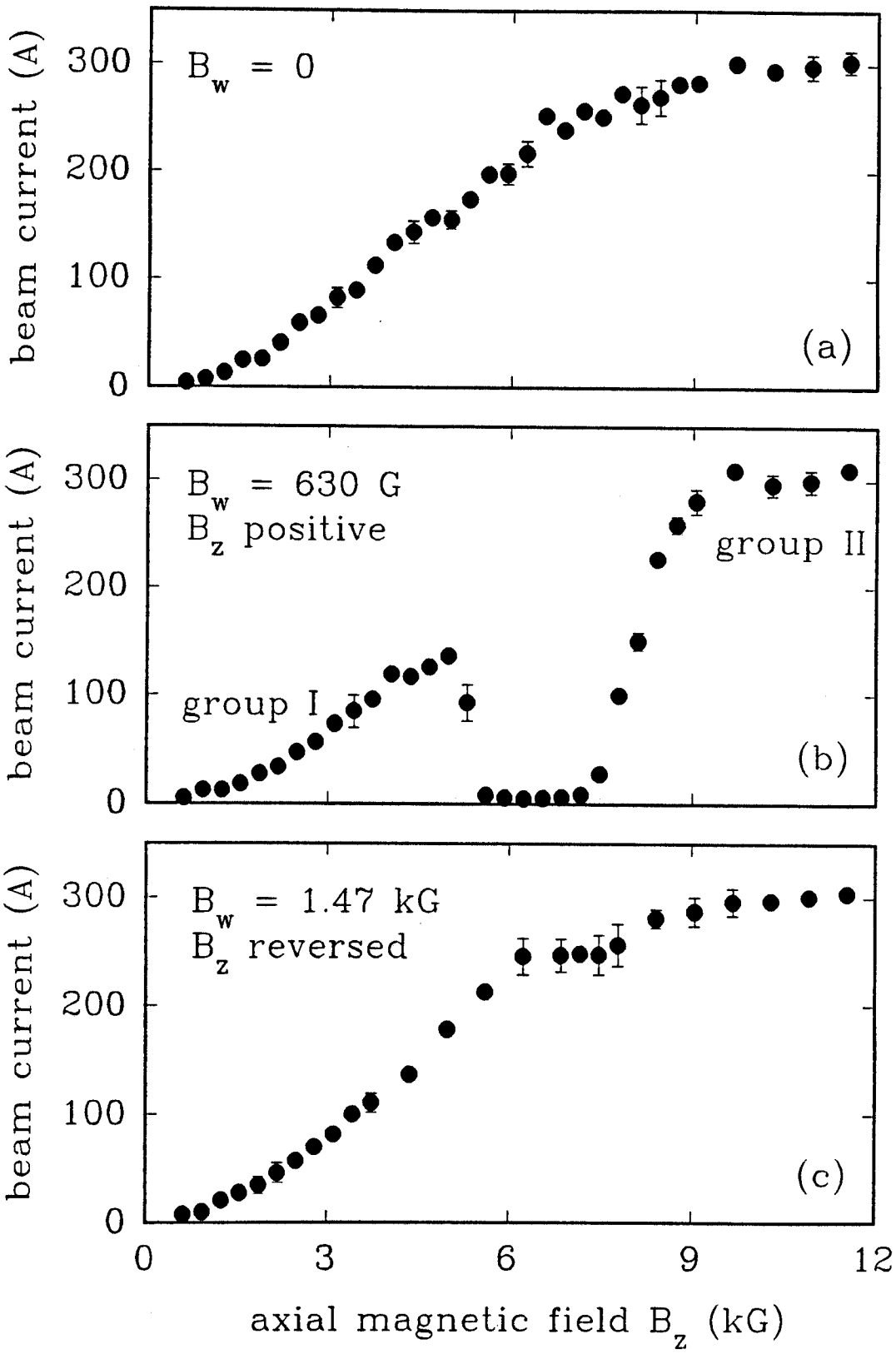

Fig.3 Conde and Bekefi

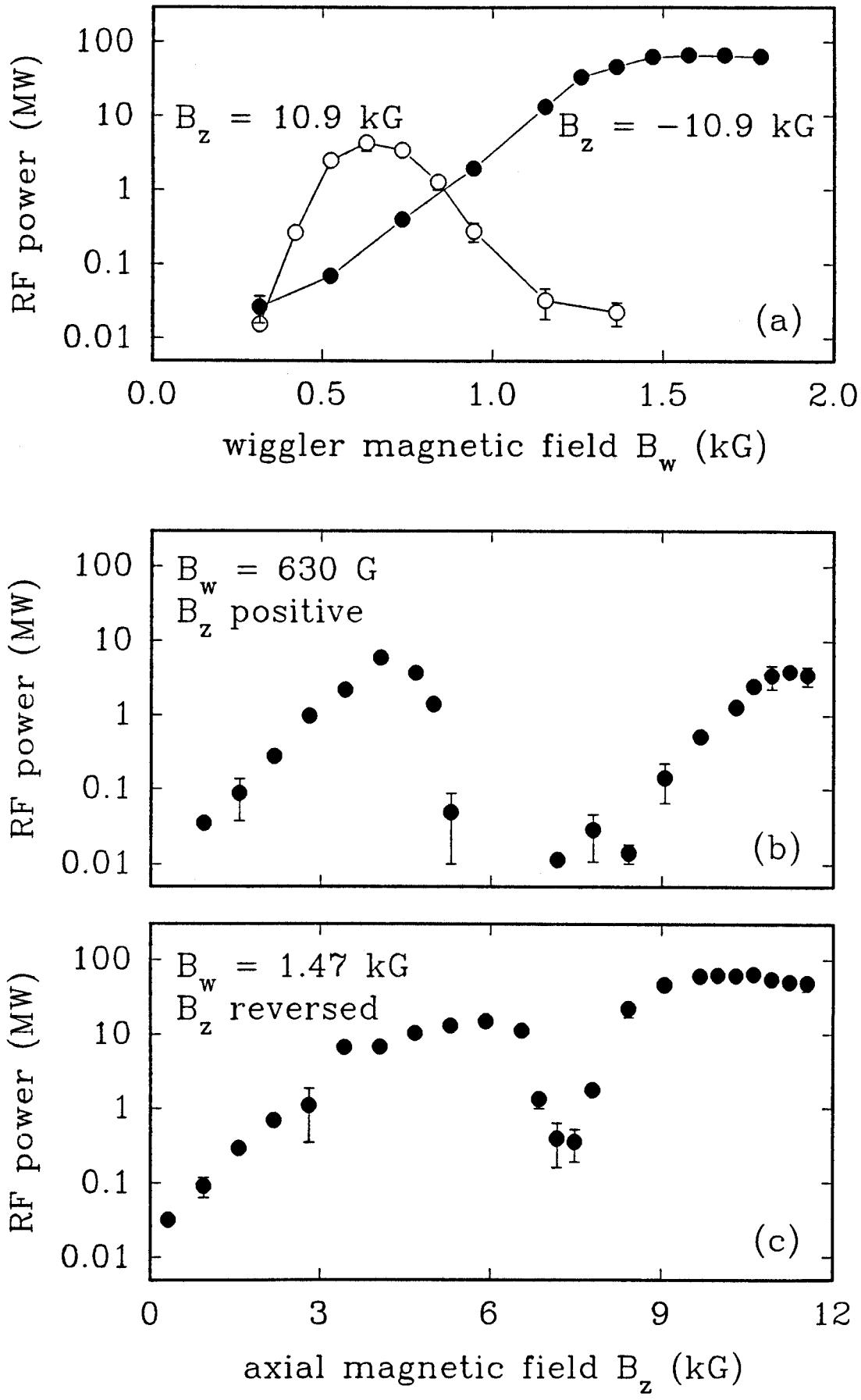

Fig.4 Conde and Bekefi

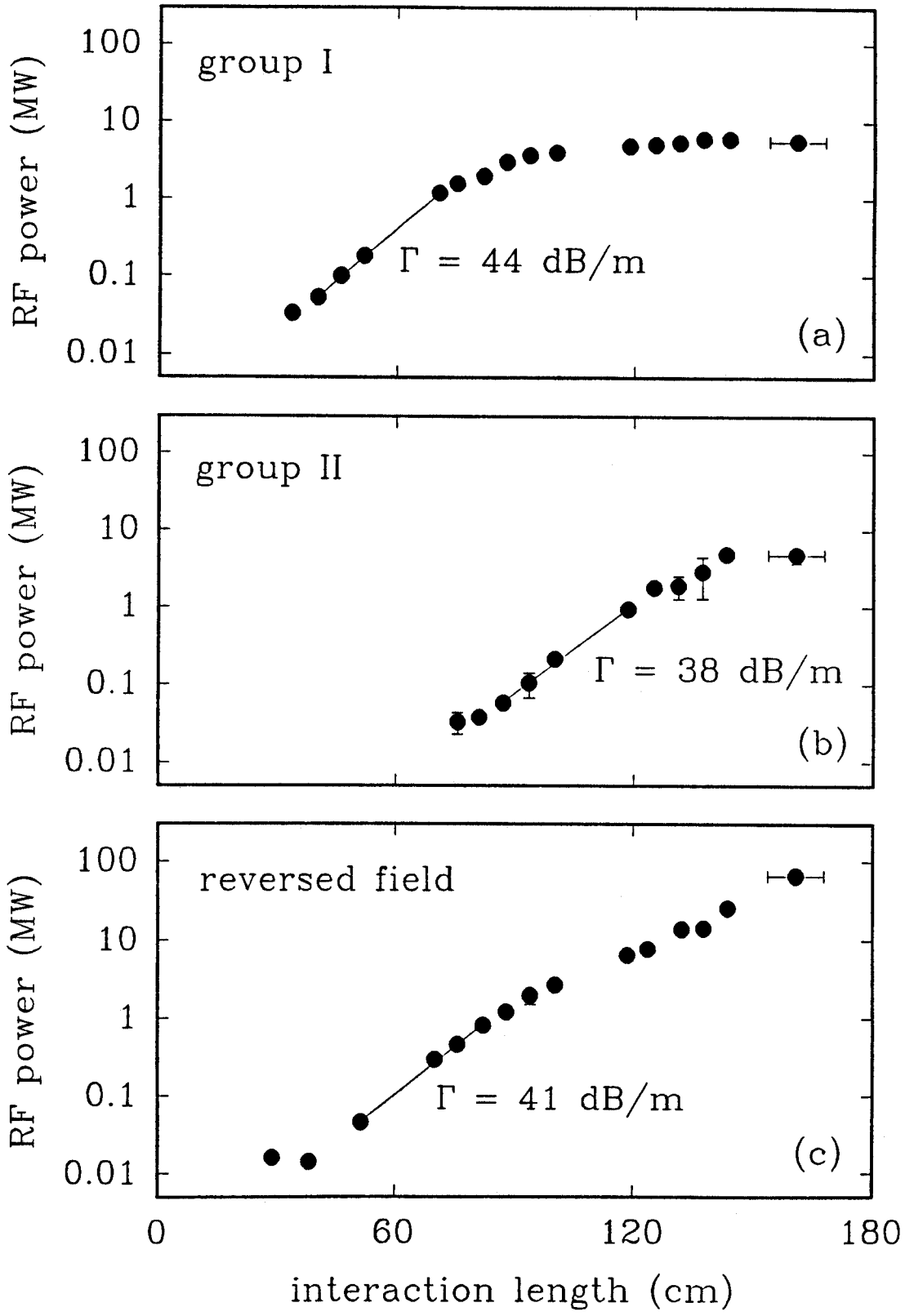

Fig.5 Conde and Bekefi